World Journal of Hepatology

Submit a Manuscript: https://www.f6publishing.com

World J Hepatol 2021 December 27; 13(12): 2052-2070

DOI: 10.4254/wjh.v13.i12.2052

ISSN 1948-5182 (online)

ORIGINAL ARTICLE

Basic Study

Gut dysbiosis and systemic inflammation promote cardiomyocyte abnormalities in an experimental model of steatohepatitis

Larisse Longo, Pabulo Henrique Rampelotto, Eduardo Filippi-Chiela, Valessa Emanoele Gabriel de Souza, Fernando Salvati, Carlos Thadeu Cerski, Themis Reverbel da Silveira, Cláudia P Oliveira, Carolina Uribe-Cruz, Mário Reis Álvares-da-Silva

ORCID number: Larisse Longo 0000-0002-4453-7227; Pabulo Henrique Rampelotto 0000-0002-8992-9697; Eduardo Filippi-Chiela 0000-0001-8192-3779; Valessa Emanoele Gabriel de Souza 0000-0002-7672-6460; Fernando Salvati 0000-0001-9331-3812; Carlos Thadeu Cerski 0000-0003-0673-5916; Themis Reverbel da Silveira 0000-0001-9867-8650; Cláudia P Oliveira 0000-0002-2848-417X; Carolina Uribe-Cruz 0000-0002-0526-3067; Mário Reis Álvares-da-Silva 0000-0002-5001-246X.

Author contributions: Longo L, Rampelotto PH, Filippi-Chiela E and Álvares-da-Silva MR performed the conceptualization, methodology, formal analysis, investigation, data curation, writing of the original draft, writing-review, and editing; de Souza VEG, Salvati F, and Cerski CT performed the conceptualization, methodology, and formal analysis; da Silveira TR, Oliveira CP and Uribe-Cruz C contributed to the conceptualization, data curation writing the original draft, writing-review and editing.

Institutional review board statement: IRB approval was obtained for this study from the Grupo de Pesquisa em Pós-

Larisse Longo, Pabulo Henrique Rampelotto, Valessa Emanoele Gabriel de Souza, Themis Reverbel da Silveira, Carolina Uribe-Cruz, Mário Reis Álvares-da-Silva, Experimental Laboratory of Hepatology and Gastroenterology, Hospital de Clínicas de Porto Alegre, Porto Alegre 90035-903, Rio Grande do Sul, Brazil

Larisse Longo, Eduardo Filippi-Chiela, Carlos Thadeu Cerski, Carolina Uribe-Cruz, Mário Reis Álvares-da-Silva, Graduate Program in Gastroenterology and Hepatology, Universidade Federal do Rio Grande do Sul, Porto Alegre 90035-003, Rio Grande do Sul, Brazil

Pabulo Henrique Rampelotto, Graduate Program in Genetics and Molecular Biology, Universidade Federal do Rio Grande do Sul, Porto Alegre 90035-903, Rio Grande do Sul, Brazil

Eduardo Filippi-Chiela, Center of Biotechnology, Universidade Federal do Rio Grande do Sul, Porto Alegre 91501-970, Rio Grande do Sul, Brazil

Eduardo Filippi-Chiela, Department of Morphological Sciences, Universidade Federal do Rio Grande do SulPorto Alegre 90050-170, Rio Grande do Sul, Brazil

Eduardo Filippi-Chiela, Experimental Research Center, Hospital de Clínicas de Porto Alegre, Porto Alegre 90035-903, Rio Grande do Sul, Brazil

Fernando Salvati, School of Medicine, Instituto Meridional de Educação-IMED, Passo Fundo 99070-220, Rio Grande do Sul, Brazil

Carlos Thadeu Cerski, Unit of Surgical Pathology, Hospital de Clínicas de Porto Alegre, Porto Alegre 90035-903, Rio Grande do Sul, Brazil

Cláudia P Oliveira, Department of Gastroenterology (LIM07), Faculdade de Medicina da Universidade de São Paulo, São Paulo 01246903, Brazil

Mário Reis Álvares-da-Silva, Division of Gastroenterology, Hospital de Clínicas de Porto Alegre, Porto Alegre 90035-903, Rio Grande do Sul, Brazil

Corresponding author: Larisse Longo, PhD, Postdoc, Experimental Laboratory of Hepatology and Gastroenterology, Hospital de Clínicas de Porto Alegre, Rua Ramiro Barcelos, 2350/Sala 12214, 2° Andar, Porto Alegre 90035-903, Rio Grande do Sul, Brazil.

Graduação – Comissão de Ética em Uso Animal do Hospital de Clí nicas de Porto Alegre.

Institutional animal care and use committee statement: All experimental procedures were approved by the Ethics Committee for the Use of Animals (No. 17-0021 and No. 17-0531) in accordance with international guidelines for animal welfare and measures were taken to minimize animal pain and discomfort.

Conflict-of-interest statement: The authors declare that they have no competing interests.

Data sharing statement: If requested and after approval, the authors authorize data sharing.

ARRIVE guidelines statement: The authors have read the ARRIVE guidelines, and the manuscript was prepared and revised according to the ARRIVE guidelines.

Country/Territory of origin: Brazil

Specialty type: Gastroenterology and hepatology

Provenance and peer review: Invited article; Externally peer reviewed.

Peer-review model: Single blind

Peer-review report's scientific quality classification

Grade A (Excellent): A
Grade B (Very good): 0
Grade C (Good): 0
Grade D (Fair): 0
Grade E (Poor): 0

larisselongo@hotmail.com

Abstract

BACKGROUND

Cardiovascular disease is the main cause of death in metabolic-associated fatty liver disease, and gut microbiota dysbiosis is associated with both of them.

AIM

To assess the relationship between gut dysbiosis and cardiovascular risk (CVR) in an experimental model of steatohepatitis.

METHODS

Adult male Sprague-Dawley rats were randomized to a control group (n = 10) fed a standard diet and an intervention group (n = 10) fed a high-fat choline-deficient diet for 16 wk. Biochemical, molecular, hepatic, and cardiac histopathology. Gut microbiota variables were evaluated.

RESULTS

The intervention group had a significantly higher atherogenic coefficient, Castelli's risk index (CRI)-I and CRI-II, interleukin-1β, tissue inhibitor of metalloproteinase-1 (all P < 0.001), monocyte chemoattractant protein-1 (P = 0.005), and plasminogen activator inhibitor-1 (P = 0.037) than the control group. Gene expression of miR-33a increased (P = 0.001) and miR-126 (P < 0.001) decreased in the intervention group. Steatohepatitis with fibrosis was seen in the intervention group, and heart computerized histological imaging analysis showed a significant decrease in the percentage of cardiomyocytes with a normal morphometric appearance (P = 0.007), reduction in the mean area of cardiomyocytes (P = 0.037), and an increase of atrophic cardiomyocytes (P = 0.007). There were significant correlations between the cardiomyocyte morphometry markers and those of progression and severity of liver disease and CVR. The intervention group had a lower Shannon diversity index and fewer changes in the structural pattern of gut microbiota (both P < 0.001) than controls. Nine microbial families that are involved in lipid metabolism were differentially abundant in intervention group and were significantly correlated with markers of liver injury and CVR.

CONCLUSION

The study found a link between gut dysbiosis and significant cardiomyocyte abnormalities in animals with steatohepatitis.

Key Words: Animal model; Cardiovascular diseases; Gut microbiota; Metabolic-associated fatty liver disease; Predicted lipid metabolism; Risk cardiovascular; Steatohepatitis

Core Tip: Cardiovascular disease is the main cause of death in metabolic-associated fatty liver disease (MAFLD) and gut microbiota dysbiosis is associated with both. Among the risk factors, we report significant correlations between the presence of atherogenic dyslipidemia, systemic inflammation, endothelial dysfunction, liver fibrogenesis, and gut dysbiosis, all of which contributed to the progression of MAFLD and increased cardiovascular risk.

Citation: Longo L, Rampelotto PH, Filippi-Chiela E, de Souza VEG, Salvati F, Cerski CT, da Silveira TR, Oliveira CP, Uribe-Cruz C, Álvares-da-Silva MR. Gut dysbiosis and systemic inflammation promote cardiomyocyte abnormalities in an experimental model of steatohepatitis. *World J Hepatol* 2021; 13(12): 2052-2070
URL: https://www.wjgnet.com/1948-5182/full/v13/i12/2052.htm
DOI: https://dx.doi.org/10.4254/wjh.v13.i12.2052

Received: April 1, 2021
Peer-review started: April 1, 2021
First decision: July 16, 2021
Revised: July 20, 2021
Accepted: October 18, 2021
Article in press: October 18, 2021
Published online: December 27, 2021

P-Reviewer: Almeida C
S-Editor: Fan JR
L-Editor: Filipodia
P-Editor: Fan JR

INTRODUCTION

Nonalcoholic fatty liver disease (NAFLD) is the most common form of liver disease and a leading cause of morbidity and mortality in both developed and developing countries[1]. The natural course the disease encompasses a pathological spectrum of liver injury ranging from simple steatosis to steatohepatitis and progressive liver fibrosis that can result in cirrhosis and other complications, including liver decompensation and hepatocellular carcinoma (HCC)[1,2]. Recently, a new nomenclature, metabolic-associated fatty liver disease (MAFLD) was suggested because the disease is not only confined to the liver only, but rather represents a major part of a multisystemic disease that includes cardiovascular manifestations[3-6]. Indeed, cardiovascular disease (CVD) is the leading cause of death in patients with MAFLD, accounting approximately 40%–45% of the total deaths[4,7,8].

The association of steatohepatitis with CVD is related to the metabolic risk factors that they have in common, such as obesity, diabetes mellitus, hypertension, and dyslipidemia. However, multiple studies have shown that steatohepatitis is also independently associated with several markers of subclinical atherosclerosis[4,7,8]. Although the putative pathophysiological mechanisms that link steatohepatitis and CVD are still not completely explained, many nontraditional and emerging risk factors, including proinflammatory cytokines and procoagulant factors (*e.g.*, fibrinogen, plasminogen, and vascular adhesion molecules) are associated with the process[7,9]. Recently, the intestinal microbiome and its highly complex and interdependent interaction with host metabolism, immunity, and disease have opened a new horizon of investigation into the link between these clinical conditions[4,9,10]. Gut microbiota, or the bacterial components and metabolites carried to the liver through the portal vein, overstimulate immune cells and may result in more severe liver damage, inflammation, and fibrosis, thus accelerating the development of steatohepatitis and inducing the systemic inflammation and endothelial dysfunction that promotes increased cardiovascular risk (CVR)[4,10]. Despite considerable progress, understanding of the molecular mechanisms governing microbiota-host interactions is far from complete. Experimental studies are needed to further explore the mechanisms whereby gut microbiota contribute to steatohepatitis-associated CVR.

The goal of this study was to assess the relationships of the gut microbiota, steatohepatitis, and CVR, by describing the crosstalk among gut dysbiosis, associated metabolic predictions, systemic inflammation, endothelial dysfunction, paracrine cell signaling, and cardiomyocyte morphology in an experimental nutritional steatohepatitis model that mimics the metabolic changes found in humans.

MATERIALS AND METHODS

Animals and experimental model

Twenty 60-day-old adult male Sprague-Dawley rats weighing 280-350 g were used. The animals were kept in groups inside two polypropylene boxes in a controlled-temperature environment (22 ± 2 °C) and a 12-h light/dark cycle. All experimental procedures were approved by the Ethics Committee for the Use of Animals (No. 17-0021 and No. 17-0531) and were conducted following the international guidelines for animal welfare. Measures were taken to minimize animal pain and discomfort.

After acclimatization to the environment, the animals were randomized to two experimental groups according to their weight, as previously described[11]. The control group (n = 10) received a standard diet (Nuvilab CR-1, Quimtia S.A., Brazil). The intervention group (n = 10) received a high-fat, choline-deficient diet consisting of 31.5% total fat and enriched with 54.0% trans fatty acids (Rhoster Ltda., Brazil) to induce steatohepatitis. Both groups received water and food ad libitum during the study. After 16 wk of treatment, the animals were fasted for 8 h, anesthetized with isoflurane, and euthanized by cardiac exsanguination. Blood samples were collected and centrifuged to obtain the serum, which was kept at −80 °C until the analyses were performed. Pieces of hepatic and cardiac tissue were fixed in 10% formaldehyde for histopathological evaluation. Feces present in the intestine were collected aseptically and kept at −80 °C for analysis of the gut microbiota.

Atherogenic ratios

Serum total cholesterol (TC), low density lipoprotein-cholesterol (LDLC), high-density lipoprotein cholesterol (HDLC) and triglycerides (TG) were assayed with a Labmax 560[11]. Atherogenic ratios were calculated from the lipid profile and used as a tool for

the prediction of CVR. The ratios included Castelli's risk index (CRI)-I = TC/HDLC, CRI-II = LDLC/HDLC and the atherogenic coefficient (AC) = (TCH − DLC)/HDLC [12].

Systemic inflammation and endothelial dysfunction

The serum markers of inflammation and endothelial dysfunction markers included in the analysis were monocyte chemoattractant protein (MCP)-1, tissue inhibitor of metalloproteinase (TIMP)-1 and plasminogen activator inhibitor (PAI)-1, and were determined by multiplex assay with the Luminex platform (Millipore, Germany). The results were expressed as ng/mL. Serum interleukin (IL)-1β was measured with an enzyme-linked immunosorbent assay kit (Thermo Scientific, United States). Absorbance was measured spectrophotometrically at a wavelength of 450 nm with a Zenyth 200rt microplate reader (Biochrom). The results were expressed in pg/mL. All procedures were performed in duplicate following the manufacturer's instructions.

Analysis of circulating microRNAs

Total RNA was extracted from serum using miRNeasy serum/plasma kits (Qiagen, United States). A cel-miR-39 (1.6×10^8 copies) spike-in control (Qiagen, United States) was added to provide an internal reference. cDNA conversion was performed with 10 ng of total RNA using TaqMan microRNA reverse transcription kits (Applied Biosystems, United States). Amplification of miR-33a, miR-126, miR-499, miR-186 and miR-146a, was performed by quantitative real-time PCR using the TaqMan assay (Applied Biosystems, United States) and expression as normalized against cell-miR-39. The sequences and codes of the assessed miRNAs are listed in Supplementary Table 1 (Private sharing link for Figshare data https://figshare.com/s/2d858620da6b13fe2fec). Values were calculated by the $2^{-(\Delta\Delta Ct)}$ method.

Hepatic histopathological analysis

Formalin-fixed liver tissue samples were embedded in paraffin, sectioned, and stained with hematoxylin and eosin (H&E) and picrosirius red. Histopathological lesions of the different evolutionary stages of liver disease were scored as previously described by Liang *et al*[13]. The score is highly reproduceable and applicable to experimental models in rodents. The analysis was performed by an experienced pathologist who was blinded to the experimental groups. Fibrosis was quantified by morphometric analysis after picrosirius red staining. Ten randomly selected fields were observed *per* animal to measure staining intensity using an Olympus BX51 microscope, and QCapture 64-bit (QImaging) at × 200 magnification. The evaluation was performed using ImageJ (version 1.51p, https://imagej.nih.gov/ij/).

Cardiomyocytes morphometric analysis

Cardiomyocyte morphometric analysis (CMA) was performed based on adaptations of the nuclear morphometric analysis developed by Filippi-Chiela *et al*[14]. Cardiomyocyte size and shape were measured using Image Pro Plus 6.0 (IPP6, Media Cybernetics). H&E images from hearts of animals were acquired. Five different fields were photographed in tissue from each animal using QCapture 64-bit software and an Olympus BX51 microscope. At least 50 cross-sectioned cardiomyocytes of each animal were analyzed. The outlines of single cells were marked using the magic wand tool of IPP6, followed by acquisition the cell area, aspect, area/box, radius ratio, and roundness. The last four measurements were used to define the cardiomyocyte irregularity index (CII) of each cell (CII = area + aspect – area/box + roundness). These variables were used to report the size and shape of single cardiomyocytes. In addition to the average size and regularity, the plot of area *vs* CMA also defined the percentage of normal, hypertrophic, and atrophic cells.

DNA extraction, 16S rRNA sequencing and bioinformatics analysis

A detailed description of the methods used for 16S ribosomal RNA gene sequencing and analyses is provided in the Supplementary Information (Private sharing link for Figshare data https://figshare.com/s/2d858620da6b13fe2fec). Briefly, after DNA extraction, the V4 hypervariable region of the 16S rRNA gene was amplified using 515F–806R primer pair and sequencing was performed with Ion Torrent (Thermo Fisher Scientific, United States). A custom pipeline in Mothur was used for 16S rRNA reads processing. Subsequent analysis of the sequence dataset and data visualization were performed in R using the vegan, phyloseq, ggplot2, and MicrobiomeAnalystR packages or QIIME.

Correlations between analyzed markers

For this analysis, we selected the histopathological NAFLD score, quantification of liver collagen, TIMP-1, MCP-1, and IL-1β as markers of severity and progression of steatohepatitis. For the correlation of CVD risk factors and lipid metabolism, we selected miR-33a, miR-126, PAI-1, CRI-I, CRI-II and AC. We selected the percentage of normal cardiomyocytes, percentage average area of cardiomyocytes, and percentages of atrophic cardiomyocyte morphological characteristics. The overall microbiota composition was correlated with the variables.

Statistical analysis

Data symmetry was tested using the Shapiro-Wilk test. Student-*t* and Mann-Whitney U tests were performed. Spearman's correlation coefficient was performed, with moderate ($0.3 < r < 0.6$), strong ($0.6 < r < 0.9$), or very strong ($0.9 < r < 1.0$) correlations. Quantitative variables were expressed as means ± standard deviation or medians with minimum and maximum values. $P \leq 0.05$ was considered statistically significant. Data were analyzed with SPSS 18.0 (IBM Corp., United States).

RESULTS

Atherogenic ratios, inflammation, and endothelial dysfunction to assess CVR

The results obtained for these parameters are shown in Table 1. There were significant increases in AC), CRI-I, and CRI-II (all $P < 0.001$) in the intervention group, indicating that the animals had an increased CVR. There were significant increases in the serum concentrations of IL-1β ($P = 0.001$), MCP-1 ($P = 0.005$), TIMP-1 ($P < 0.001$), and PAI-1 ($P = 0.037$) in the intervention group compared with the control group. Together, the results suggest the study intervention had increased systemic inflammation and endothelial dysfunction.

Level of circulating microRNAs related to CVR

The levels of circulating microRNAs related to CVR are shown in Figure 1. There was a significant increase in the gene expression of miR-33a ($P = 0.001$) in the intervention group compared with the control group, the opposite was reported for miR-126 ($P < 0.001$). There were no between-group differences in the expression of miR-499 ($P = 0.171$), miR-186 ($P = 0.151$), and miR-146a ($P = 0.151$).

Liver histopathological analysis

No abnormalities were seen in the livers of the control group animals, whereas animals in the intervention group had predominantly microvesicular steatosis along with macrovesicular steatosis of moderate intensity, inflammatory activity, and a mild degree of fibrosis. In the histopathological staging of lesions, seven animals in the intervention group had steatohepatitis and three had simple steatosis. Picrosirius red staining of collagen was more intense ($P < 0.001$) in animals in the intervention group than in the control group (4.10, range: 3.02-6.04 *vs* 1.35, range: 1.21-1.55) relative luminescence units, indicating a significant increase in the deposition of connective tissue fibers in the liver.

Morphometric and histopathological evaluation of cardiomyocytes

Myocardial steatosis was not observed in either the control of intervention group. The evaluation of cardiomyocyte morphometry (*i.e.* size and shape) demonstrated the percentages of normal size, large, or small cells and their shape regularity (Figure 2A). There was a significant decrease in the percentage of cardiomyocytes with a normal morphometric appearance ($P = 0.007$) in the intervention group compared with the control group (Figure 2B). Among the most clinically relevant morphometric changes, there was a significant reduction in the mean area of cardiomyocytes ($P = 0.037$, Figure 2C) and a significant increase in the percentage of atrophic cardiomyocytes in the intervention group ($P = 0.007$, Figure 2D) in relation to the control group. Finally, we separated the animals in the intervention group into two subgroups by the median percentages of normal cardiomyocytes (Figure 2E) and atrophic cardiomyocytes (Figure 2F) and the average area (Figure 2G) and then compared the data. Animals with a percentage of normal cardiomyocytes higher than the median had higher liver tissue levels of TIMP-1, IL-1β, IL-6 and myeloid differentiation primary response (Myd)-88, and lower levels of IL-1β/IL-10 (Figure 2E). Animals with a percentage of atrophic cardiomyocytes above the median had lower liver tissue levels of IL-1β

Table 1 Atherogenic ratios, inflammation and endothelial dysfunction markers in a nutritional model of steatohepatitis

Variable	Control (*n* = 10)	Intervention (*n* = 10)	*P* value
AC	0.6 (0.2–0.9)	2.5 (1.5–3.4)	< 0.001[a]
CRI-I	1.6 (± 0.4)	3.5 (± 1.1)	< 0.001[a]
CRI-II	0.3 (± 0.1)	0.8 (± 0.2)	< 0.001[a]
IL-1β (pg/mL)	367.7 (± 31.2)	465.9 (± 52.7)	0.001[a]
MCP-1 (ng/mL)	2.7 (± 0.6)	3.8 (± 0.9)	0.005[a]
TIMP-1 (ng/mL)	7.1 (± 1.4)	12.4 (± 2.3)	< 0.001[a]
PAI-1 (ng/mL)	0.11 (± 0.05)	0.17 (± 0.06)	0.037[a]

Data are means ± standard deviation or medians (25^{th}-75^{th} percentiles).

[a]$P \leq 0.05$ was considered statistically significant.

AC: Atherogenic coefficient; CRI: Castelli's risk index; IL: Interleukin; MCP: Monocyte chemoattractant protein; PAI: Plasminogen activator inhibitor; TIMP: Tissue inhibitor of metalloproteinase.

(Figure 2F). Animals with an average cardiomyocytes area greater than the median had lower liver tissue levels of tumor necrosis factor-α/IL-10 (Figure 2G).

Gut microbiota diversity and composition

The Shannon diversity index was significantly lower ($P < 0.001$) in intervention than in the control group (Figure 3A). In addition, analysis of similarities (ANOSIM) revealed that the structural pattern of the gut microbiota in intervention group was clearly distinct from that of the control group ($P < 0.001$) by principal coordinates analysis (PCoA) using the Bray-Curtis distance metric (Figure 3B). In terms of composition (*i.e.* taxonomic identification), 1266 bacterial taxa (operational taxonomic units) that belonged to 112 genera, 41 families, and eight phyla were identified. *Firmicutes* (53.1%) and *Bacteroidetes* (43.1%) were the most abundant phyla in all samples. The most abundant families were *Muribaculaceae* (21.7%), *Lachnospiraceae* (20.8%), *Ruminococcaceae* (18.5%), and *Bacteroidaceae* (15.4%, Figure 3C). The four families represented 76.4% of all observed taxa. Differential abundance analysis identified nine families that were associated with the intervention group and one family associated with control group (Linear discriminant analysis score > 2.0; Figure 3D).*Bacteroidaceae*, *Ruminococcaceae*, *Peptostreptococcaceae*, *Peptococcaceae*, *Erysipelotricaceae*, *Clostridiaceae*, *B- urkholderiaceae*, *Streptococcaeae*, and *Tannerellaceae* were differentially abundant in the intervention group. *Lachnospiraceae* was differentially abundant in control group. The distribution of the 41 families and their features are shown in Figure 3E. Most of the taxa prevalent in control group were less prevalent or absent in intervention group. The reverse was also observed.

Lipid metabolism prediction

PCoA using the Bray-Curtis distance metric indicated that the clustering of the predicted lipid metabolic pathways in the study groups was clearly distinct (ANOSIM, $P < 0.001$) As shown in Figure 4A, two samples, R01 and R11, were considered outliers and were not included in further statistical analysis (*e.g.*, LefSe analysis). The distribution of the predicted lipid metabolic pathways is shown in Figure 4B. In total, 12 metabolic pathways were identified in which the between-group difference in the relative frequency was significant ($P < 0.001$, linear discriminant analysis score > 2.0; Figure 4C). The results showed that metabolic pathways involved in sphingolipid metabolism, fatty acid biosynthesis, fatty acid metabolism, steroid hormone biosynthesis, and arachidonic acid metabolism were significantly increased in intervention group, and glycerophospholipid metabolism, glycerolipid metabolism, synthesis and degradation of ketone bodies, biosynthesis of unsaturated fatty acids, alpha-linolenic acid metabolism, linoleic acid metabolism, and ether lipid metabolism were significantly increased in control group.

Correlations between steatohepatitis, CVR, and gut microbiota

The correlations between markers of liver disease progression and severity, CVR factors, cardiomyocyte morphometry and microbiota composition are shown in Table 2. Additional correlations can be found in Supplementary Table 2 (Private

Table 2 Correlation of steatohepatitis, cardiovascular risk, and microbiota composition

Variable[1]		Severity and progression of liver injury				CVR factors and metabolism of lipids						Cardiomyocyte morphometry			Microbiota composition
		Quantification of collagen (picrosirius)	TIMP-1	MCP-1	IL-1β	miR-33a	miR-126	PAI-1	CRI-I	CRI-II	AC	% Normal CAR	Average area of CAR	% Atrophic CAR	
Severity and progression of liver injury	**NAFLD score**	0.879[2]	0.791[2]	0.673[2]	0.347	0.639[2]	-0.777[2]	0.444[3]	0.809[2]	0.820[2]	0.809[2]	-0.519[3]	-0.630[2]	0.721[2]	0.694[2]
	Quantification of collagen (picrosirius)		0.611[2]	0.456[3]	0.752[2]	0.571[3]	-0.683[2]	0.415	0.819[2]	0.821[2]	0.819[2]	-0.205	-0.312	0.238	0.378[2]
	TIMP-1			0.803[2]	0.726[2]	0.728[2]	-0.812[2]	0.535[3]	0.691[2]	0.747[2]	0.691[2]	-0.694[2]	-0.405	0.607[2]	0.539[2]
	MCP-1				0.567[3]	0.492[3]	-0.623[2]	0.336	0.549[3]	0.561[3]	0.549[3]	-0.490[3]	-0.390	0.498[3]	0.232[3]
	IL-1β					0.809[2]	-0.688[3]	0.544[3]	0.645[3]	0.688[2]	0.645[3]	-0.437[3]	-0.393	0.382	0.293[3]
CVR factors and metabolism of lipids	**miR-33a**						-0.655[2]	0.363	0.529[3]	0.603[3]	0.529[3]	-0.704[2]	0.038	0.232	0.160[3]
	miR-126							-0.634[2]	-0.712[2]	-0.730[2]	-0.712[2]	0.459[3]	0.320	-0.364	0.368[2]
	PAI-1								0.487[3]	0.671[2]	0.487[3]	-0.317	0.389	-0.289	0.103
	CRI-I									0.863[2]	1.000[2]	-0.234	-0.459[3]	0.386	0.469[2]
	CRI-II										0.863[2]	-0.399	-0.492[3]	0.551[3]	0.584[2]
	AC											-0.236	-0.457[3]	0.389	0.477[2]
Cardiomyocyte morphometry	**% Normal cardiomyocytes**												0.105	-0.058	
	% Average area of cardiomyocytes													-0.818[2]	
	% Atrophic cardiomyocytes														

[1]Variables were evaluated by Spearman's *r* correlation coefficient: moderate ($0.3 < r < 0.6$), strong ($0.6 < r < 0.9$) or very strong ($0.9 < r < 1.0$).

[2]Correlation significant at the 0.01 level.

[3]Correlation significant at the 0.05 level.

AC: Atherogenic coefficient; CAR: Cardiomyocytes; CRI: Castelli's risk index; CVR: Cardiovascular risk; IL: Interleukin; MCP: Monocyte chemoattractant protein; NAFLD: Nonalcoholic fatty liver disease; PAI: Plasminogen activator inhibitor; TIMP: Tissue inhibitor of metalloproteinase.

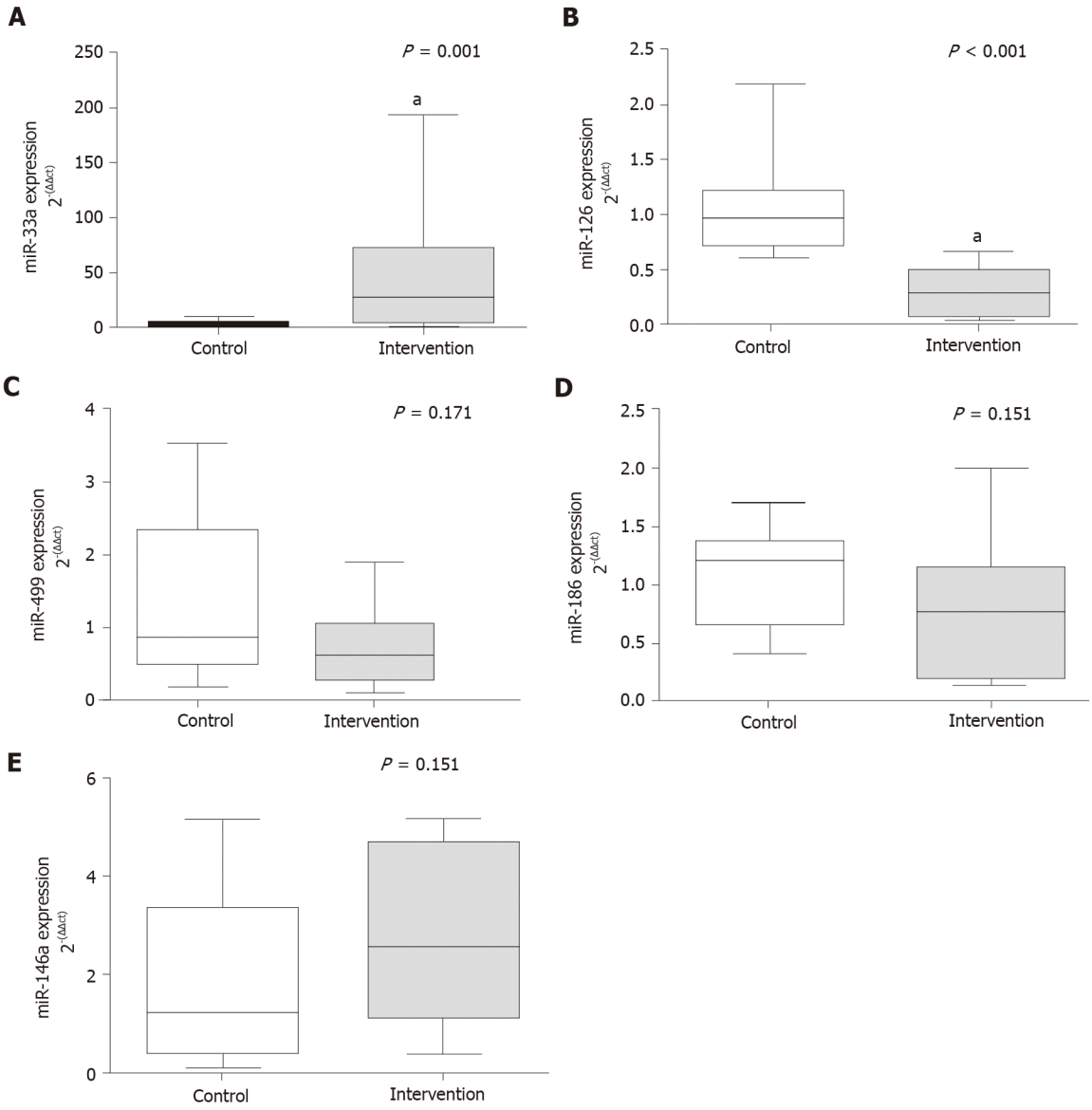

Figure 1 Gene expression of circulating microRNAs. A: miR-33a ($P = 0.001$); B: miR-126 ($P < 0.001$); C: miR-499 ($P = 0.171$); D: miR-186 ($P = 0.151$); E: miR-146a ($P = 0.151$). $^{a}P < 0.05$, Significant effect of the high-fat and choline-deficient diet. Data are medians (25th-75th percentile), Mann-Whitney U test.

sharing link for Figshare data https://figshare.com/s/2d858620da6b13fe2fec). There was a positive correlation between the markers of steatohepatitis severity and progression with CVR factors, such as miR-33a, PAI-1, and atherogenic ratios. Negative correlations were observed for miR-126. Regarding cardiomyocyte morphometry, there were negative correlations between the average area and the percentage of normal cardiomyocytes with the NAFLD score. There was a positive correlation of histopathological NAFLD score with the percentage of atrophic cardiomyocytes, a negative correlation between the percentage of normal cardiomyocytes with MCP-1 and TIMP-1 and a positive correlation of those markers with the percentage of atrophic cardiomyocytes. Furthermore, the average area of cardiomyocytes correlated negatively with atherogenic ratios, CRI-I, CRI-II and AC. miR-33a correlated negatively and miR-126 and positively with the percentage of normal cardiomyocytes.

The composition of the microbiota was positively correlated with markers of liver injury and CVR. The correlation of each family of microorganisms with markers of liver disease progression and severity and CVR factors are shown in Table 3. Significant moderate and strong correlations were observed between nearly all families of bacteria and the hepatic histopathology score, collagen fiber deposition in hepatic tissue, TIMP-1, microRNAs, and atherogenic ratios. Families of interest in the underlying disease including *Bacteroidaceae*, *Clostridiaceae*, *Firmicutes* and *Lactobacillaceae* were correlated with the evaluated markers. No correlation was observed

Table 3 Correlation of gut microbiota at family level, steatohepatitis, and cardiovascular risk factors

Variable[1] (Family)	Severity and progression of liver injury				CVR factors and metabolism of lipids					
	NAFLD score	Quantification of collagen (picrosirius)	TIMP-1	MCP-1	miR-33a	miR-126	PAI-1	CRI-I	CRI-II	AC
Actinomycetaceae					0.584[2]					
Aerococcaceae										
Anaeroplasmataceae		-0.553[2]						-0.614[2]		-0.614[2]
Atopobiaceae	0.627[2]	0.610[2]						0.592[2]	0.663[2]	0.592[2]
Bacillales_unclassified						0.549[2]		-0.548[2]	-0.533[2]	-0.548[2]
Bacteroidaceae	0.836[2]	0.746[2]	0.784[2]		0.689[2]	-0.754[2]		0.662[2]	0.732[2]	0.662[2]
Bacteroidales_unclassified		-0.560[2]							-0.589[2]	-0.492[2]
Burkholderiaceae									0.564[2]	
Clostridiaceae	0.807[2]	0.723[2]	0.645[2]		0.593[2]	-0.669[2]		0.676[2]	0.638[2]	0.676[2]
Clostridiales_unclassified	-0.628[2]	-0.529[2]	-0.535[2]		-0.576[2]				-0.586[2]	-0.525[2]
Clostridiales_vadinBB60	-0.602[2]	-0.671[2]	-0.527[2]		-0.558[2]	0.524[2]		-0.626[2]	-0.502[2]	-0.626[2]
Corynebacteriaceae	-0.669[2]	-0.545[2]	-0.680[2]		-0.782[2]	0.611[2]		-0.571[2]	-0.622[2]	-0.571[2]
Desulfovibrionaceae	-0.806[2]	-0.603[2]	-0.872[2]	-0.776[2]	-0.631[2]	0.755[2]		-0.729[2]	-0.746[2]	-0.729[2]
Eggerthellaceae									0.490[2]	
Firmicutes_unclassified	-0.797[2]	-0.637[2]	-0.687[2]		-0.655[2]	0.594[2]		-0.629[2]	-0.699[2]	-0.629[2]
Gastranaerophilales	-0.822[2]	-0.656[2]	-0.644[2]		-0.643[2]	0.657[2]		-0.698[2]	-0.586[2]	-0.698[2]
Lachnospiraceae	-0.850[2]	-0.653[2]	-0.789[2]	-0.788[2]	-0.613[2]	0.766[2]		-0.643[2]	-0.629[2]	-0.643[2]
Lactobacillaceae	-0.616[2]	-0.633[2]				0.795[2]			-0.529[2]	
Lactobacillales_unclassified										
Micrococcaceae	0.669[2]		0.534[2]			-0.528[2]			0.493[2]	
Mollicutes_RF39_fa	-0.650[2]	-0.618[2]	-0.590[2]		-0.609[2]	0.713[2]		-0.857[2]	-0.768[2]	-0.857[2]
Moraxellaceae	-0.669[2]	-0.536[2]	-0.557[2]		-0.543[2]			-0.599[2]	-0.473[2]	-0.599[2]
Muribaculaceae	-0.816[2]	-0.794[2]			-0.576[2]	0.693[2]	-0.684[2]	-0.827[2]	-0.846[2]	-0.827[2]
Pasteurellaceae										
Prevotellaceae		-0.705[2]				0.603[2]			-0.522[2]	-0.486[2]

Rikenellaceae				-0.679[2]				
Saccharimonadaceae	-0.737[2]	-0.559[2]	-0.619[2]	-0.674[2]	0.656[2]	-0.776[2]	-0.759[2]	-0.776[2]
Staphylococcaceae	-0.734[2]	-0.647[2]	-0.808[2]	-0.838[2]	0.716[2]	-0.616[2]	-0.679[2]	-0.616[2]
Streptococcaceae	0.790[2]	0.726[2]	0.637[2]	0.595[2]	-0.622[2]		0.724[2]	0.515[2]

[1]Variables were evaluated by Spearman's *r* correlation coefficient, moderate ($0.3 < r < 0.6$) or strong ($0.6 < r < 0.9$).
[2]Correlation significant at the 0.05 level.
AC: Atherogenic coefficient; CRI: Castelli's risk index; CVR: Cardiovascular risk; MCP: Monocyte chemoattractant protein; NAFLD: Nonalcoholic fatty liver disease; PAI: Plasminogen activator inhibitor; TIMP: Tissue inhibitor of metalloproteinase.

between families of gut microbiota and measurements of cardiomyocyte morphometry.

DISCUSSION

Steatohepatitis and CVD are both associated with metabolic risk factors, including glucose abnormalities, dyslipidemia, chronic inflammation, endothelial dysfunction, and gut dysbiosis. The relationship is recognized in the clinical setting, but the links among steatohepatitis, CVD, and gut dysbiosis needs to be better understood. This study provided evidence of the role of MAFLD as an adjuvant risk factor for the development of CVD. We found that dysbiotic bacteria and their metabolites were translocated to the liver through the ruptured intestinal barrier, causing impaired hepatic triglyceride metabolism, inflammatory responses, and fibrogenesis, which are necessary for the development and progression of MAFLD[11]. We also found significant correlations between the activation of pathophysiological pathways that link MAFLD and increased risk of developing cardiovascular events, such as atherogenic dyslipidemia, systemic inflammation, endothelial dysfunction, gut dysbiosis, and changes in cardiomyocyte morphometry. In this study, the significant associations between steatohepatitis and CVR, justify the screening of MAFLD and its associated risk factors in high-risk patients, in order to intervene effectively, with a focus on new approaches aimed at directing the composition of the intestinal microbiota as a potential therapeutic target.

In a recent publication, we reported that the experimental nutritional model developed in this study is capable of causing marked deposition of body and liver fat, changes in biochemical parameters, activation of microRNAs, receptors, mediators, and inflammatory cytokines, an increase in intestinal permeability, and hepatic histopathological changes, similar to steatohepatitis in humans[11]. This robust experimental model of steatohepatitis of metabolic origin allows evaluating pathophysiological mechanisms related to the development of CVD in MAFLD. We

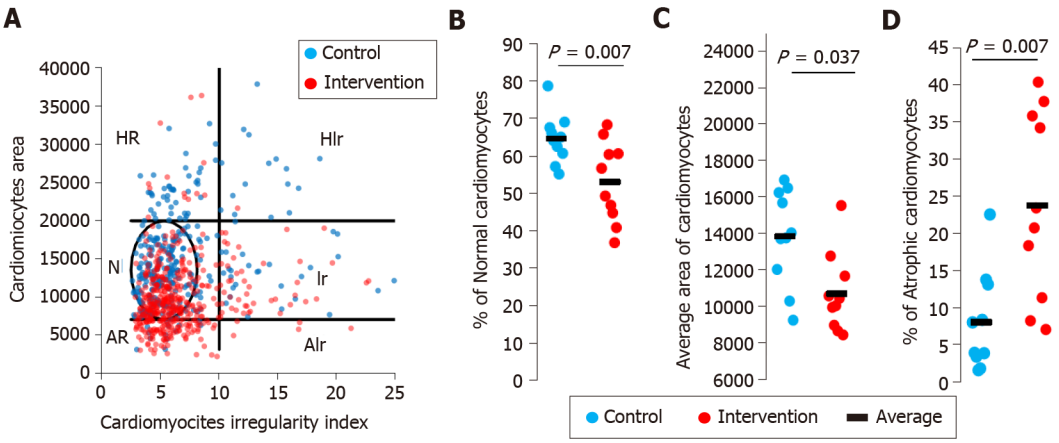

E

% Normal cardiomyocytes	TIMP-1	IL-1β	Myd88	IL-6 (liver)	IL-1β/IL-10 (liver)
< Median	13.5	3.9	7.3	52914	0.52
> Median	11.2	1.1	2.9	45436	0.64
T Test	0.05	0.04	0.04	0.02	0.01

F

% Atrophic cardiomyocytes	IL-1β (liver)
< Median	2560
> Median	3309
T Test	0.003

G

Average area	TNF-α/IL-10 (liver)
< Median	2.3
> Median	3.4
T Test	0.028

Figure 2 Cardiomyocytes morphometric analysis. The area and cross-sectional shape of cardiomyocytes were determined from images of hematoxylin and eosin-stained tissue. A: Dot plot of cardiomyocyte area *vs* cardiomyocyte irregularity index in control (blue) and intervention (red) groups. Each dot represents a population of cardiomyocytes with different morphometry. N–normal area and shape, Ir–normal area and irregular shape, HR–hypertrophic and regular cardiomyocytes, HIr–hypertrophic and irregular cardiomyocytes, AR–atrophic and regular cardiomyocytes, AIr–atrophic and irregular cardiomyocyte; B: Average area of cardiomyocytes; C: Percentage of normal cardiomyocytes; D: Percentage of atrophic cardiomyocytes; E-G: We segregated the animals in the intervention group into two subgroups and the data were compared. IL: Interleukin; TNF: Tumor necrosis factor.

demonstrated that abnormalities of lipid metabolism and atherogenic ratios were related to greater propensity to develop CVD associated with steatohepatitis. The results are consistent with other experimental and clinical studies[7,15-18]. In addition, we report a significant increase of systemic markers of inflammation and endothelial dysfunction in animals with steatohepatitis. The worsening of the inflammatory state in MAFLD is associated with worse cardiometabolic outcomes. PAI-1 is a marker of endothelial dysfunction, being released in response to low-grade inflammation, free fatty acids, and atherogenic lipoproteins[19,20]. A previous study reporting that an increase in PAI-1 was correlated with the histological severity of MAFLD and alterations in the lipid profile, promoting a more atherogenic phenotype[21]. PAI-1 also plays a vital role in liver fibrosis, promoting increased deposition of extracellular matrix in liver tissue, in which TIMP-1 performs a similar function[22]. In that sense, liver fibrosis can lead to severe hepatic dysfunction and even life-threatening conditions such as liver cirrhosis and HCC. The mechanism of liver fibrosis is multifaceted and, in this study, animals with steatohepatitis had an increase in TIMP-1 concentration and deposition of collagen fibers in liver tissue, markers that significantly correlated with increased CVR.

Assessment of microRNAs has been used for the early detection and monitoring of the progression of MAFLD, and to assess clinical and subclinical CVD. miR-33a inhibits genes involved in high-density lipoprotein synthesis and the reverse transport of cholesterol[23,24]. In this study, animals with steatohepatitis had a significant increase in miR-33a expression that was positively correlated with atherogenic ratios and markers of severity and progression of liver injury. miR-126 expression, which is high in endothelial cells and regulates the migration of inflammatory cells, formation of capillary networks, and cell survival[25], was decreased in animals with steatohepatitis. In fact, there was an inverse correlation between miR-126 expression and


A
Shannon index
4.0
3.5
3.0
B
Control
Intervention
Axis.2 [12.6%]
0.8
0.4
0
-0.4
-0.8
-0.50
-0.25
0.00
0.25
0.50
Axis.1 [45.7%]
C
Control
Intervention
Relative abundance
1.00
0.75
0.50
0.25
0.00
R01 R02 R03 R04 R05 R06 R07 R08 R09 R10
R11 R12 R13 R14 R15 R16 R17 R18 R19 R20
Family
Bacteroidaceae
Muribaculaceae
Lachnospiraceae
Ruminococcaceae
Peptococcaceae
Others
Peptostreptococcaceae
Rikenellaceae
Erysipelotrichaceae
Clostridiaceae_1
D
Control
Bacteroidaceae
Ruminococcaceae
Peptostreptococcaceae
Peptococcaceae
Erysipelotrichaceae
Clostridiaceae_1
Burkholderiaceae
Streptococcaceae
Tannerellaceae
Christensenellaceae
Desulfovibrionaceae
Gastranaerophilales_fa
Lachnospiraceae
Intervention
-5
-4
-3
-2
-1
0
1
2
3
4
5
LDA score

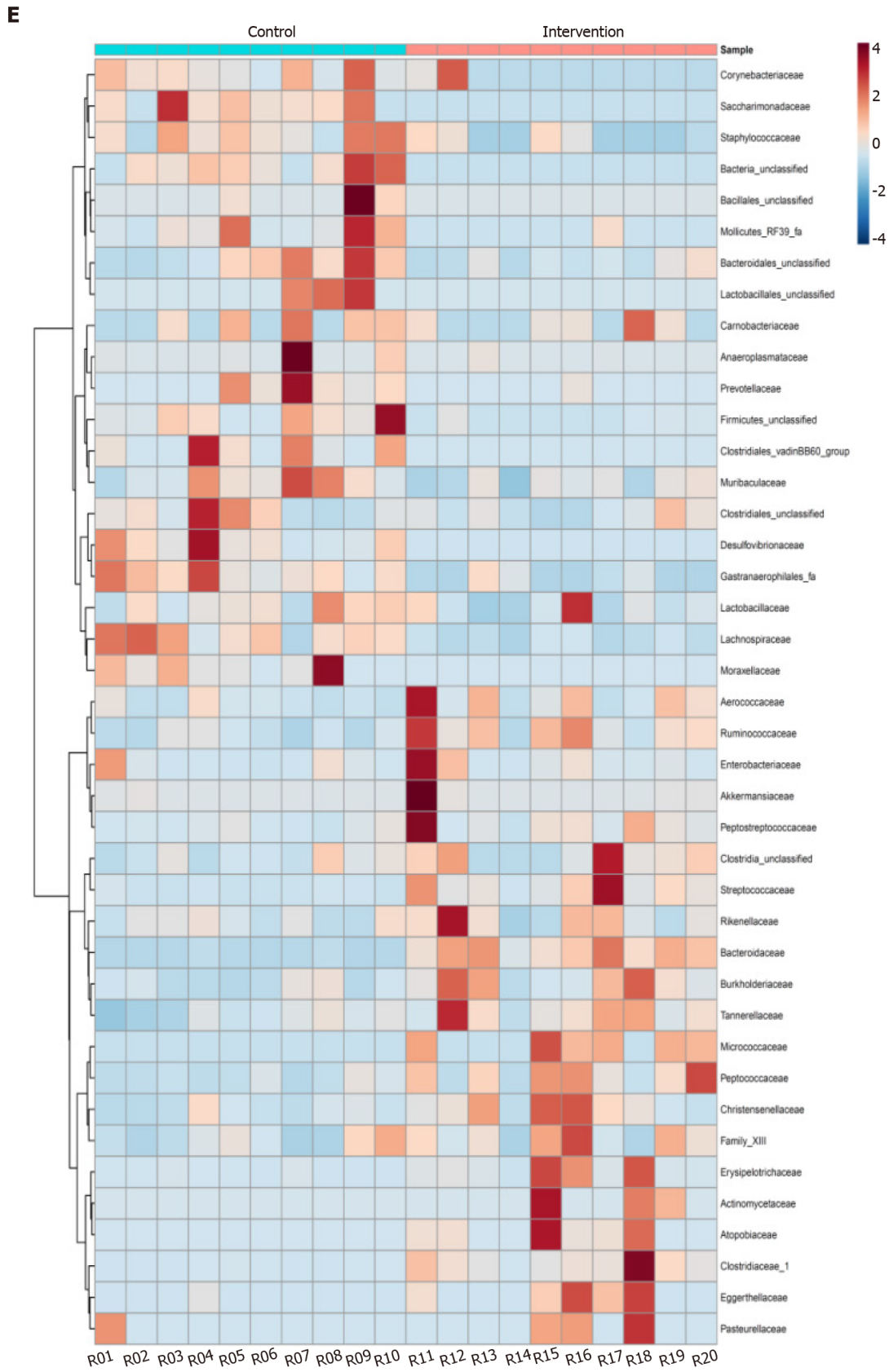

Figure 3 Gut microbiota changes in intervention and control groups. A: Shannon diversity index; B: Principal coordinate analysis based on Bray-Curtis distance metric; C: Relative abundance of gut microbiota at the family level; D: Differential abundance by linear discriminant analysis; E: Heatmap distribution of the 41 families among the samples. LDA: Linear discriminant analysis.

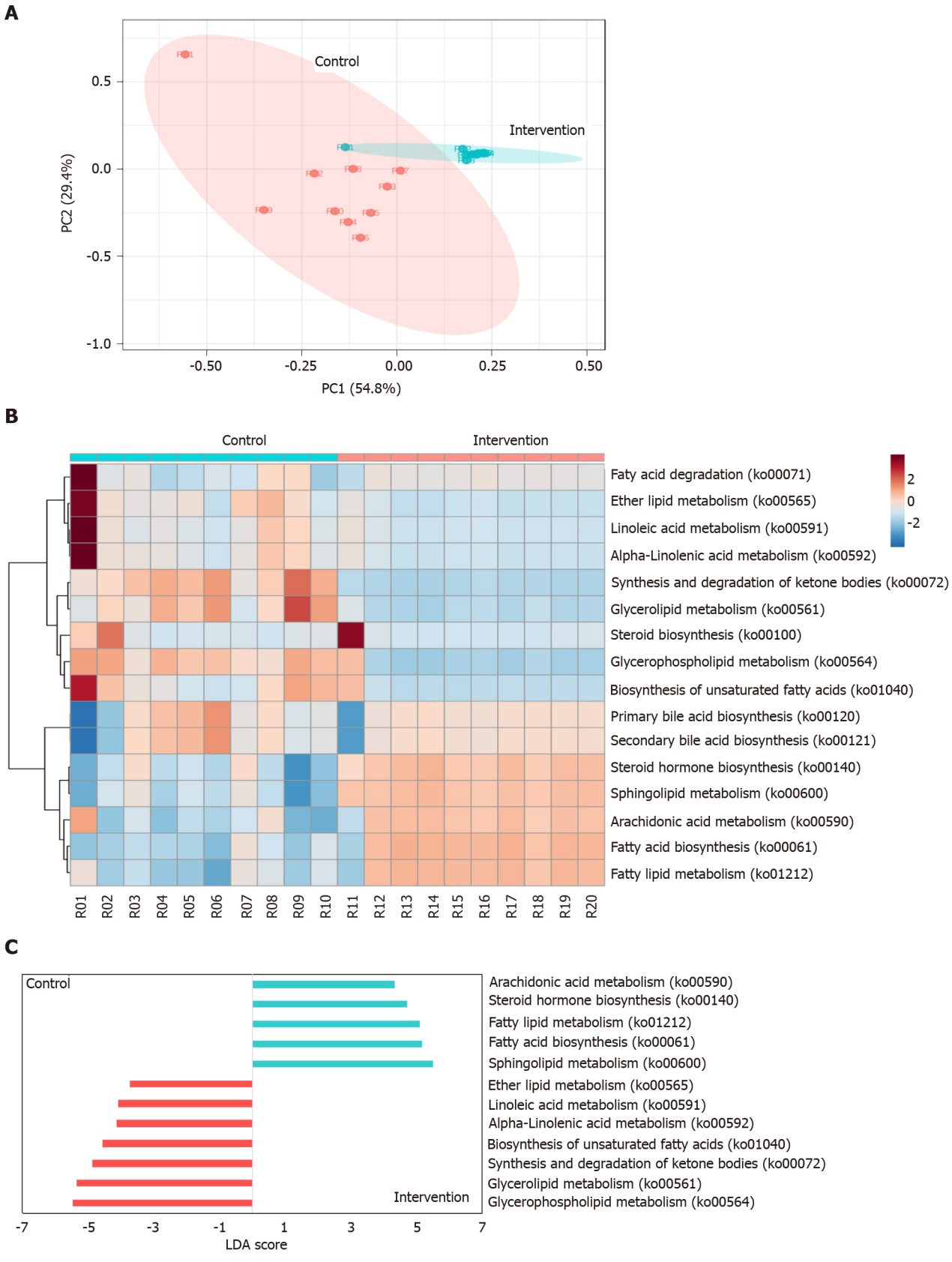

Figure 4 Sixteen predicted functional Kyoto Encyclopedia of Genes and Genomes lipid metabolism pathways in intervention and control group. A: Principal coordinate analysis; B: Heatmap distribution; C: Linear discriminant analysis (LDA) of the 16 differentially abundant KEGG lipid metabolism pathways.

atherogenic ratios, endothelial dysfunction, inflammation, fibrogenesis, and severity of liver injury. As established in the literature, microRNAs act in the epigenetic regulation of intricate processes[24,25]. In this study, we clearly demonstrated that the

expression of miR-33a and miR-126 was involved in the regulation of cholesterol, lipid metabolism, and endothelial dysfunction, and contributed to the development of metabolic disorders and CVD related to steatohepatitis.

The morphometric evaluation of cardiomyocytes was an interesting and innovative analysis in this study, and it found that animals with steatohepatitis had a significant decreases in the percentage of cardiomyocytes with a normal appearance and the mean area of cardiomyocytes relative to the control group. In addition, animals with steatohepatitis had a significant increase in the percentage of atrophic cardiomyocytes. To the best of our knowledge, morphometric analysis of cardiomyocytes in MAFLD has not been previously reported, which makes it difficult to discuss the data obtained. Several cellular processes can be inferred through morphometric analysis, and the method can be used in the diagnosis and prognosis of some clinical conditions[14,26,27]. In this study, we reported that the percentage of normal cardiomyocytes was negatively correlated with the histological severity of liver damage, fibrogenesis, and inflammation. Furthermore, the percentage of atrophic cardiomyocytes correlated positively with the liver injury markers. Clinical manifestations of MAFLD, such as steatosis and inflammation, are additional risk factors for the development of CVD[3,9]. However, the exact mechanisms for this complex relationship are unclear[3,9]. It is likely that several highly interrelated factors contribute to the increase of CVR in steatohepatitis and changes in the morphometry of cardiomyocytes. However, more studies are needed to evaluate the morphometry of cardiomyocytes in more advanced stages of MAFLD.

The "multiple parallel hits" hypothesis highlights the importance of the gut microbiota and seems to provide a more accurate explanation of the pathogenesis of steatohepatitis and its contribution to the increase in CVR[3,10]. The liver is closely related to the intestine both anatomically and functionally, and recent evidence demonstrates that the type and quantity of intestinal microorganisms determine important characteristics related to the pathogenesis and progression of these clinical conditions[28-30]. Our data corroborate with experimental and clinical studies reporting that the development and progression of MAFLD is associated with a significant decrease in the diversity and structure of the bacterial communities of the gut microbiota[29,31,32]. In this study, we report an increase in the abundance of family *Bacteroidaceae* and a decrease in the abundance of *Prevotellaceae* in animals with steatohepatitis. It is known that the diet directly influences the composition of the gut microbiota. Western diets abundant in fat, animal protein, and sugar have been associated with steatohepatitis and increased risk of CVD. That diet favors the abundance of family *Bacteroidaceae*; while diets high in fiber, starch, and plant polysaccharides promote the abundance of family *Prevotellaceae*[30,33,34]. In this study, we report an increase in the abundance of family *Bacteroidaceae* and a decrease in the abundance of *Prevotellaceae* in animals with steatohepatitis, which is consistent with another study[30]. Regarding the increase in the relative abundance of family *Ruminococcacea* observed in the animals of the intervention group, a previous report that demonstrated the *Ruminococcus increased* in more severe disease, especially if advanced hepatic fibrosis was diagnosed. The decrease in its abundance has also been reported in lean steatohepatitis patients[30,35]. There are reports that associate the abundance of *Ruminococcaceae* with the development of CVD[36,37]. However, we found no correlations between the presence of *Ruminococcaceae* and the CVR markers that were assessed in this study. Genus *Ruminococcus* is quite heterogeneous, including both beneficial and deleterious bacteria, making data discussion difficult. Family *Ruminococcaceae* is associated with aerobic fermentation that leads to the production of short chain fatty acids and alcohol, and this can have detrimental effects on intestinal permeability and hepatic inflammation[30,35].

Some of the metabolites produced by gut flora are already biologically active, whereas others are further metabolized by the host, generating secondary mediators that influence the microbiota-host interaction. In this study, we predicted the lipid metabolic pathways that were expressed as a result of the gut dysbiosis observed in steatohepatitis. Animals with steatohepatitis had a significant increase in sphingolipid metabolism. The sphingolipids are membrane lipids that participate in cell division, differentiation, gene expression, and apoptosis. The study data corroborate emerging evidence that support the role of sphingolipids in hepatocellular death, which contributes to the progression of MAFLD[38]. Additionally, there are reports that dysregulation of circulating sphingolipids was independently associated with CVD and subclinical atherosclerosis[39,40]. In this study, arachidonic acid metabolism was significantly increased in animals with steatohepatitis. In addition, a significant decrease in linoleic acid metabolism was reported in this experimental group. Arachidonic acid is synthesized from polyunsaturated fatty acids, and can be derived

from linoleic acid, which is an essential fatty acid[41]. The products resulting from arachidonic acid metabolism are linked to the inflammation and vasodilation of MAFLD and CVD, mainly by the action of the enzyme cyclooxygenase[41,42]. Therefore, as reported in this study, an increase in arachidonic acid metabolism in steatohepatitis and CVD is expected. We report an increase in glycerophospholipid metabolism in animals in the control group. As described by Schnabl and Brenner[43], a high-fat diet causes the gut microbiota to convert choline in the diet to methylamines, consequently reducing the plasma levels of phosphatidylcholine, which is a glycerophospholipid. Phosphatidylcholine is an important constituent of the cell membrane of very low density lipoproteins. Without its presence triglycerides cannot attach to the lipoprotein and start to accumulate in the liver tissue, causing MAFLD [43]. In parallel, there were increases in plasma trimethylamine, and its hepatic metabolism to trimethylamine-N-oxide has been associated with the appearance of CVD. This compound is considered harmful, as it changes the way cholesterol and steroids are metabolized and inhibits the reverse transport of cholesterol, causing the accumulation of fat on the internal walls of arteries[44,45]. Therefore, in this study, the predicted lipid metabolism in animals with steatohepatitis did not include expression of glycerophospholipid metabolism, probably because of the action of the gut microbiota in the metabolic pathway.

CONCLUSION

In summary, it is known that steatohepatitis and CVD have many risk factors in common. Among those, we report significant correlations between the presence of atherogenic dyslipidemia, systemic inflammation, endothelial dysfunction, liver fibrogenesis, and gut dysbiosis, all of which contribute to the progression of MAFLD and increased CVR. In addition, we infer, through the composition of the gut microbiota, which lipid metabolism pathways are activated in animals with steatohepatitis and their relationship with CVR. Subsequent metabolomic studies may aid in elucidating the influence of gut microbial function with the development of cardiometabolic disorders related to steatohepatitis. The gut microbiota may be a potential therapeutic target for both clinical conditions.

ARTICLE HIGHLIGHTS

Research background

Metabolic-associated fatty liver disease (MAFLD), in addition to being a progressive liver disease, is an independent and significant risk factor for the development of cardiovascular disease, and dysbiosis of the intestinal microbiota is associated with both.

Research motivation

The motivation was to explore the mechanisms whereby gut microbiota contribute to steatohepatitis-associated increased cardiovascular risk.

Research objectives

The objective was to assess the relationship between gut dysbiosis and cardiovascular risk in an experimental model of steatohepatitis.

Research methods

Adult male Sprague-Dawley rats were randomized to a control group given a standard diet or an intervention of a high-fat and choline-deficient diet for 16 wk of ten animals each. Biochemical, molecular, hepatic, and cardiac histopathology and gut microbiota variables were evaluated.

Research results

We reported significant correlations between the presence of atherogenic dyslipidemia, systemic inflammation, endothelial dysfunction, liver fibrogenesis and gut dysbiosis, all of which contributed to the progression of MAFLD and increased CVR.

Research conclusions

This study shows that there is a link between gut dysbiosis and significant cardiomyocyte abnormalities in animals with steatohepatitis.

Research perspectives

Metabolomic studies may aid in elucidating the association of gut microbial function with the development of cardiometabolic disorders related to steatohepatitis. The gut microbiota may be a potential therapeutic target for both clinical conditions.

ACKNOWLEDGEMENTS

The authors would like to thank the Hospital de Clínicas de Porto Alegre, CNPq (National Counsel of Technological and Scientific Development), PNPD/CAPES (Coordination for the Improvement of Higher Education Personnel) Program.

REFERENCES

1 **Younossi Z**, Anstee QM, Marietti M, Hardy T, Henry L, Eslam M, George J, Bugianesi E. Global burden of NAFLD and NASH: trends, predictions, risk factors and prevention. *Nat Rev Gastroenterol Hepatol* 2018; **15**: 11-20 [PMID: 28930295 DOI: 10.1038/nrgastro.2017.109]

2 **Estes C**, Razavi H, Loomba R, Younossi Z, Sanyal AJ. Modeling the epidemic of nonalcoholic fatty liver disease demonstrates an exponential increase in burden of disease. *Hepatology* 2018; **67**: 123-133 [PMID: 28802062 DOI: 10.1002/hep.29466]

3 **El Hadi H**, Di Vincenzo A, Vettor R, Rossato M. Cardio-Metabolic Disorders in Non-Alcoholic Fatty Liver Disease. *Int J Mol Sci* 2019; **20** [PMID: 31064058 DOI: 10.3390/ijms20092215]

4 **Anstee QM**, Mantovani A, Tilg H, Targher G. Risk of cardiomyopathy and cardiac arrhythmias in patients with nonalcoholic fatty liver disease. *Nat Rev Gastroenterol Hepatol* 2018; **15**: 425-439 [PMID: 29713021 DOI: 10.1038/s41575-018-0010-0]

5 **Eslam M**, Sanyal AJ, George J; International Consensus Panel. MAFLD: A Consensus-Driven Proposed Nomenclature for Metabolic Associated Fatty Liver Disease. *Gastroenterology* 2020; **158**: 1999-2014.e1 [PMID: 32044314 DOI: 10.1053/j.gastro.2019.11.312]

6 **Eslam M**, Newsome PN, Sarin SK, Anstee QM, Targher G, Romero-Gomez M, Zelber-Sagi S, Wai-Sun Wong V, Dufour JF, Schattenberg JM, Kawaguchi T, Arrese M, Valenti L, Shiha G, Tiribelli C, Yki-Järvinen H, Fan JG, Grønbæk H, Yilmaz Y, Cortez-Pinto H, Oliveira CP, Bedossa P, Adams LA, Zheng MH, Fouad Y, Chan WK, Mendez-Sanchez N, Ahn SH, Castera L, Bugianesi E, Ratziu V, George J. A new definition for metabolic dysfunction-associated fatty liver disease: An international expert consensus statement. *J Hepatol* 2020; **73**: 202-209 [PMID: 32278004 DOI: 10.1016/j.jhep.2020.03.039]

7 **Choudhary NS**, Duseja A. Screening of Cardiovascular Disease in Nonalcoholic Fatty Liver Disease: Whom and How? *J Clin Exp Hepatol* 2019; **9**: 506-514 [PMID: 31516267 DOI: 10.1016/j.jceh.2019.02.005]

8 **Niederseer D**, Wernly S, Bachmayer S, Wernly B, Bakula A, Huber-Schönauer U, Semmler G, Schmied C, Aigner E, Datz C. Diagnosis of Non-Alcoholic Fatty Liver Disease (NAFLD) Is Independently Associated with Cardiovascular Risk in a Large Austrian Screening Cohort. *J Clin Med* 2020; **9** [PMID: 32283679 DOI: 10.3390/jcm9041065]

9 **Francque SM**, van der Graaff D, Kwanten WJ. Non-alcoholic fatty liver disease and cardiovascular risk: Pathophysiological mechanisms and implications. *J Hepatol* 2016; **65**: 425-443 [PMID: 27091791 DOI: 10.1016/j.jhep.2016.04.005]

10 **Ji Y**, Yin Y, Li Z, Zhang W. Gut Microbiota-Derived Components and Metabolites in the Progression of Non-Alcoholic Fatty Liver Disease (NAFLD). *Nutrients* 2019; **11** [PMID: 31349604 DOI: 10.3390/nu11081712]

11 **Longo L**, Tonin Ferrari J, Rampelotto PH, Hirata Dellavia G, Pasqualotto A, P Oliveira C, Thadeu Schmidt Cerski C, Reverbel da Silveira T, Uribe-Cruz C, Álvares-da-Silva MR. Gut Dysbiosis and Increased Intestinal Permeability Drive microRNAs, NLRP-3 Inflammasome and Liver Fibrosis in a Nutritional Model of Non-Alcoholic Steatohepatitis in Adult Male Sprague Dawley Rats. *Clin Exp Gastroenterol* 2020; **13**: 351-368 [PMID: 32982365 DOI: 10.2147/CEG.S262879]

12 **Sujatha R**, Kavitha S. Atherogenic indices in stroke patients: A retrospective study. *Iran J Neurol* 2017; **16**: 78-82 [PMID: 28761629]

13 **Liang W**, Menke AL, Driessen A, Koek GH, Lindeman JH, Stoop R, Havekes LM, Kleemann R, van den Hoek AM. Establishment of a general NAFLD scoring system for rodent models and comparison to human liver pathology. *PLoS One* 2014; **9**: e115922 [PMID: 25535951 DOI: 10.1371/journal.pone.0115922]

14 **Filippi-Chiela EC**, Oliveira MM, Jurkovski B, Callegari-Jacques SM, da Silva VD, Lenz G. Nuclear morphometric analysis (NMA): screening of senescence, apoptosis and nuclear irregularities. *PLoS*

One 2012; **7**: e42522 [PMID: 22905142 DOI: 10.1371/journal.pone.0042522]
15 **Siddiqui MS**, Fuchs M, Idowu MO, Luketic VA, Boyett S, Sargeant C, Stravitz RT, Puri P, Matherly S, Sterling RK, Contos M, Sanyal AJ. Severity of nonalcoholic fatty liver disease and progression to cirrhosis are associated with atherogenic lipoprotein profile. *Clin Gastroenterol Hepatol* 2015; **13**: 1000-8.e3 [PMID: 25311381 DOI: 10.1016/j.cgh.2014.10.008]
16 **Targher G**, Lonardo A, Byrne CD. Nonalcoholic fatty liver disease and chronic vascular complications of diabetes mellitus. *Nat Rev Endocrinol* 2018; **14**: 99-114 [PMID: 29286050 DOI: 10.1038/nrendo.2017.173]
17 **Lee HS**, Nam Y, Chung YH, Kim HR, Park ES, Chung SJ, Kim JH, Sohn UD, Kim HC, Oh KW, Jeong JH. Beneficial effects of phosphatidylcholine on high-fat diet-induced obesity, hyperlipidemia and fatty liver in mice. *Life Sci* 2014; **118**: 7-14 [PMID: 25445436 DOI: 10.1016/j.lfs.2014.09.027]
18 **Taher J**, Baker C, Alvares D, Ijaz L, Hussain M, Adeli K. GLP-2 Dysregulates Hepatic Lipoprotein Metabolism, Inducing Fatty Liver and VLDL Overproduction in Male Hamsters and Mice. *Endocrinology* 2018; **159**: 3340-3350 [PMID: 30052880 DOI: 10.1210/en.2018-00416]
19 **Kodaman N**, Aldrich MC, Sobota R, Asselbergs FW, Brown NJ, Moore JH, Williams SM. Plasminogen Activator Inhibitor-1 and Diagnosis of the Metabolic Syndrome in a West African Population. *J Am Heart Assoc* 2016; **5** [PMID: 27697752 DOI: 10.1161/JAHA.116.003867]
20 **Chang ML**, Lin YS, Pao LH, Huang HC, Chiu CT. Link between plasminogen activator inhibitor-1 and cardiovascular risk in chronic hepatitis C after viral clearance. *Sci Rep* 2017; **7**: 42503 [PMID: 28211910 DOI: 10.1038/srep42503]
21 **Jin R**, Krasinskas A, Le NA, Konomi JV, Holzberg J, Romero R, Vos MB. Association between plasminogen activator inhibitor-1 and severity of liver injury and cardiovascular risk in children with non-alcoholic fatty liver disease. *Pediatr Obes* 2018; **13**: 23-29 [PMID: 27764892 DOI: 10.1111/ijpo.12183]
22 **Barrera F**, George J. Prothrombotic factors and nonalcoholic fatty liver disease: an additional link to cardiovascular risk? *Hepatology* 2014; **59**: 16-18 [PMID: 23787943 DOI: 10.1002/hep.26588]
23 **Horie T**, Nishino T, Baba O, Kuwabara Y, Nakao T, Nishiga M, Usami S, Izuhara M, Sowa N, Yahagi N, Shimano H, Matsumura S, Inoue K, Marusawa H, Nakamura T, Hasegawa K, Kume N, Yokode M, Kita T, Kimura T, Ono K. MicroRNA-33 regulates sterol regulatory element-binding protein 1 expression in mice. *Nat Commun* 2013; **4**: 2883 [PMID: 24300912 DOI: 10.1038/ncomms3883]
24 **Koyama S**, Horie T, Nishino T, Baba O, Sowa N, Miyasaka Y, Kuwabara Y, Nakao T, Nishiga M, Nishi H, Nakashima Y, Nakazeki F, Ide Y, Kimura M, Tsuji S, Ruiz Rodriguez R, Xu S, Yamasaki T, Otani C, Watanabe T, Nakamura T, Hasegawa K, Kimura T, Ono K. Identification of Differential Roles of MicroRNA-33a and -33b During Atherosclerosis Progression With Genetically Modified Mice. *J Am Heart Assoc* 2019; **8**: e012609 [PMID: 31242815 DOI: 10.1161/JAHA.119.012609]
25 **Alique M**, Bodega G, Giannarelli C, Carracedo J, Ramírez R. MicroRNA-126 regulates Hypoxia-Inducible Factor-1α which inhibited migration, proliferation, and angiogenesis in replicative endothelial senescence. *Sci Rep* 2019; **9**: 7381 [PMID: 31089163 DOI: 10.1038/s41598-019-43689-3]
26 **Beck AH**, Sangoi AR, Leung S, Marinelli RJ, Nielsen TO, van de Vijver MJ, West RB, van de Rijn M, Koller D. Systematic analysis of breast cancer morphology uncovers stromal features associated with survival. *Sci Transl Med* 2011; **3**: 108ra113 [PMID: 22072638 DOI: 10.1126/scitranslmed.3002564]
27 **Bugrova ML**, Abrosimov DA, Ermolin IL. Ultrastructural Morphological Characterization of Right Atrial and Left Ventricular Rat Cardiomyocytes during Postreperfusion Period. *Bull Exp Biol Med* 2017; **163**: 805-808 [PMID: 29063323 DOI: 10.1007/s10517-017-3908-6]
28 **Lim S**, Taskinen MR, Borén J. Crosstalk between nonalcoholic fatty liver disease and cardiometabolic syndrome. *Obes Rev* 2019; **20**: 599-611 [PMID: 30589487 DOI: 10.1111/obr.12820]
29 **Ezzaidi N**, Zhang X, Coker OO, Yu J. New insights and therapeutic implication of gut microbiota in non-alcoholic fatty liver disease and its associated liver cancer. *Cancer Lett* 2019; **459**: 186-191 [PMID: 31185249 DOI: 10.1016/j.canlet.2019.114425]
30 **Boursier J**, Mueller O, Barret M, Machado M, Fizanne L, Araujo-Perez F, Guy CD, Seed PC, Rawls JF, David LA, Hunault G, Oberti F, Calès P, Diehl AM. The severity of nonalcoholic fatty liver disease is associated with gut dysbiosis and shift in the metabolic function of the gut microbiota. *Hepatology* 2016; **63**: 764-775 [PMID: 26600078 DOI: 10.1002/hep.28356]
31 **Gómez-Zorita S**, Aguirre L, Milton-Laskibar I, Fernández-Quintela A, Trepiana J, Kajarabille N, Mosqueda-Solís A, González M, Portillo MP. Relationship between Changes in Microbiota and Liver Steatosis Induced by High-Fat Feeding-A Review of Rodent Models. *Nutrients* 2019; **11** [PMID: 31505802 DOI: 10.3390/nu11092156]
32 **Demir M**, Lang S, Martin A, Farowski F, Wisplinghoff H, Vehreschild MJGT, Krawczyk M, Nowag A, Scholz CJ, Kretzschmar A, Roderburg C, Lammert F, Goeser T, Kasper P, Steffen HM. Phenotyping non-alcoholic fatty liver disease by the gut microbiota: Ready for prime time? *J Gastroenterol Hepatol* 2020; **35**: 1969-1977 [PMID: 32267559 DOI: 10.1111/jgh.15071]
33 **De Filippo C**, Cavalieri D, Di Paola M, Ramazzotti M, Poullet JB, Massart S, Collini S, Pieraccini G, Lionetti P. Impact of diet in shaping gut microbiota revealed by a comparative study in children from Europe and rural Africa. *Proc Natl Acad Sci U S A* 2010; **107**: 14691-14696 [PMID: 20679230 DOI: 10.1073/pnas.1005963107]
34 **Yatsunenko T**, Rey FE, Manary MJ, Trehan I, Dominguez-Bello MG, Contreras M, Magris M, Hidalgo G, Baldassano RN, Anokhin AP, Heath AC, Warner B, Reeder J, Kuczynski J, Caporaso JG,

Lozupone CA, Lauber C, Clemente JC, Knights D, Knight R, Gordon JI. Human gut microbiome viewed across age and geography. *Nature* 2012; **486**: 222-227 [PMID: 22699611 DOI: 10.1038/nature11053]

35 **Duarte SMB**, Stefano JT, Miele L, Ponziani FR, Souza-Basqueira M, Okada LSRR, de Barros Costa FG, Toda K, Mazo DFC, Sabino EC, Carrilho FJ, Gasbarrini A, Oliveira CP. Gut microbiome composition in lean patients with NASH is associated with liver damage independent of caloric intake: A prospective pilot study. *Nutr Metab Cardiovasc Dis* 2018; **28**: 369-384 [PMID: 29482963 DOI: 10.1016/j.numecd.2017.10.014]

36 **Kurilshikov A**, van den Munckhof ICL, Chen L, Bonder MJ, Schraa K, Rutten JHW, Riksen NP, de Graaf J, Oosting M, Sanna S, Joosten LAB, van der Graaf M, Brand T, Koonen DPY, van Faassen M; LifeLines DEEP Cohort Study, BBMRI Metabolomics Consortium, Slagboom PE, Xavier RJ, Kuipers F, Hofker MH, Wijmenga C, Netea MG, Zhernakova A, Fu J. Gut Microbial Associations to Plasma Metabolites Linked to Cardiovascular Phenotypes and Risk. *Circ Res* 2019; **124**: 1808-1820 [PMID: 30971183 DOI: 10.1161/CIRCRESAHA.118.314642]

37 **Toya T**, Corban MT, Marrietta E, Horwath IE, Lerman LO, Murray JA, Lerman A. Coronary artery disease is associated with an altered gut microbiome composition. *PLoS One* 2020; **15**: e0227147 [PMID: 31995569 DOI: 10.1371/journal.pone.0227147]

38 **Yue F**, Xia K, Wei L, Xing L, Wu S, Shi Y, Lam SM, Shui G, Xiang X, Russell R, Zhang D. Effects of constant light exposure on sphingolipidomics and progression of NASH in high-fat-fed rats. *J Gastroenterol Hepatol* 2020; **35**: 1978-1989 [PMID: 32027419 DOI: 10.1111/jgh.15005]

39 **Jiang XC**, Paultre F, Pearson TA, Reed RG, Francis CK, Lin M, Berglund L, Tall AR. Plasma sphingomyelin level as a risk factor for coronary artery disease. *Arterioscler Thromb Vasc Biol* 2000; **20**: 2614-2618 [PMID: 11116061 DOI: 10.1161/01.atv.20.12.2614]

40 **Nelson JC**, Jiang XC, Tabas I, Tall A, Shea S. Plasma sphingomyelin and subclinical atherosclerosis: findings from the multi-ethnic study of atherosclerosis. *Am J Epidemiol* 2006; **163**: 903-912 [PMID: 16611667 DOI: 10.1093/aje/kwj140]

41 **Farrell GC**, Haczeyni F, Chitturi S. Pathogenesis of NASH: How Metabolic Complications of Overnutrition Favour Lipotoxicity and Pro-Inflammatory Fatty Liver Disease. *Adv Exp Med Biol* 2018; **1061**: 19-44 [PMID: 29956204 DOI: 10.1007/978-981-10-8684-7_3]

42 **Futosi K**, Fodor S, Mócsai A. Reprint of Neutrophil cell surface receptors and their intracellular signal transduction pathways. *Int Immunopharmacol* 2013; **17**: 1185-1197 [PMID: 24263067 DOI: 10.1016/j.intimp.2013.11.010]

43 **Schnabl B**, Brenner DA. Interactions between the intestinal microbiome and liver diseases. *Gastroenterology* 2014; **146**: 1513-1524 [PMID: 24440671 DOI: 10.1053/j.gastro.2014.01.020]

44 **Zhao ZH**, Xin FZ, Zhou D, Xue YQ, Liu XL, Yang RX, Pan Q, Fan JG. Trimethylamine N-oxide attenuates high-fat high-cholesterol diet-induced steatohepatitis by reducing hepatic cholesterol overload in rats. *World J Gastroenterol* 2019; **25**: 2450-2462 [PMID: 31171889 DOI: 10.3748/wjg.v25.i20.2450]

45 **Dumas ME**, Kinross J, Nicholson JK. Metabolic phenotyping and systems biology approaches to understanding metabolic syndrome and fatty liver disease. *Gastroenterology* 2014; **146**: 46-62 [PMID: 24211299 DOI: 10.1053/j.gastro.2013.11.001]

Published by **Baishideng Publishing Group Inc**
7041 Koll Center Parkway, Suite 160, Pleasanton, CA 94566, USA
Telephone: +1-925-3991568
E-mail: bpgoffice@wjgnet.com
Help Desk: https://www.f6publishing.com/helpdesk
https://www.wjgnet.com